Article

Cancer Cell

UNR/CSDE1 Drives a Post-transcriptional Program to Promote Melanoma Invasion and Metastasis

Graphical Abstract

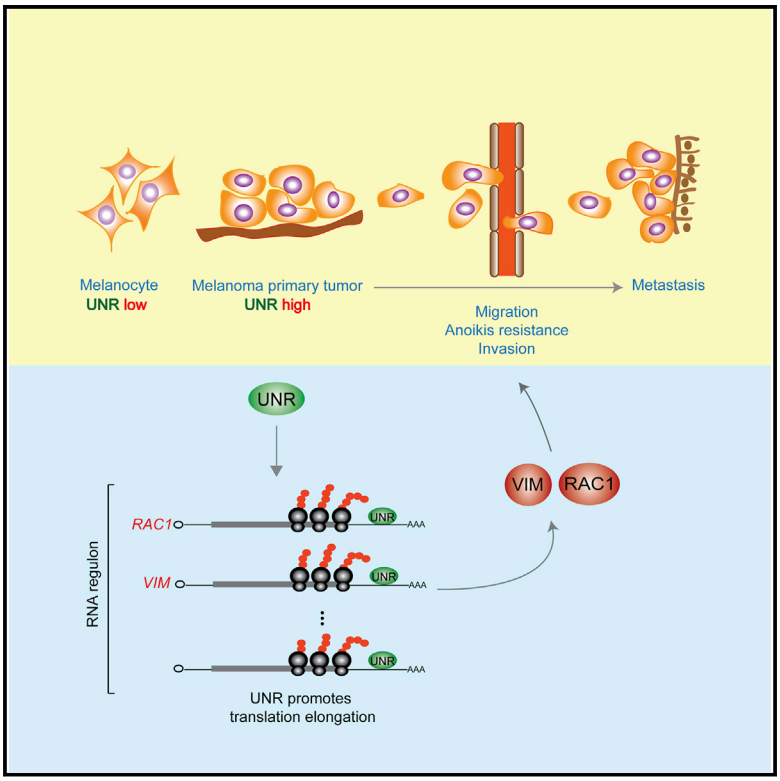

Authors

Laurence Wurth,
Panagiotis Papasaikas,
David Olmeda, ..., Stefan Hüttelmaier,
Maria S. Soengas, Fátima Gebauer

Correspondence

fatima.gebauer@crg.eu

In Brief

Wurth et al. find that the RNA binding protein UNR is often overexpressed in melanoma and promotes invasion and metastasis. Using iCLIP-seq, RNA-seq, and ribosome profiling, the authors identify potentially oncogenic RNA regulons, one of which includes RAC1 and VIM, whose translation is regulated by UNR.

Highlights

- UNR promotes melanoma invasion and metastasis
- UNR coordinates novel pro-metastatic RNA regulons
- UNR regulates translation elongation of Vimentin and RAC1 mRNAs
- UNR controls the steady-state levels of PTEN mRNA

Wurth et al., 2016, Cancer Cell *30*, 694–707
November 14, 2016
http://dx.doi.org/10.1016/j.ccell.2016.10.004

CellPress

Cancer Cell
Article

UNR/CSDE1 Drives a Post-transcriptional Program to Promote Melanoma Invasion and Metastasis

Laurence Wurth,[1,2] Panagiotis Papasaikas,[1,2] David Olmeda,[3] Nadine Bley,[4] Guadalupe T. Calvo,[3] Santiago Guerrero,[1,2] Daniela Cerezo-Wallis,[3] Javier Martinez-Useros,[5] María García-Fernández,[3] Stefan Hüttelmaier,[4] Maria S. Soengas,[3] and Fátima Gebauer[1,2,6,*]

[1]Gene Regulation, Stem Cells and Cancer Programme, Centre for Genomic Regulation (CRG), The Barcelona Institute of Science and Technology, 08003 Barcelona, Spain
[2]Universitat Pompeu Fabra (UPF), 08003 Barcelona, Spain
[3]Molecular Oncology Programme, Spanish National Cancer Research Centre (CNIO), 28029 Madrid, Spain
[4]Section Molecular Cell Biology, Institute of Molecular Medicine (IMM), Martin-Luther-University (MLU), 06120 Halle, Germany
[5]Translational Oncology Division, Oncohealth Institute - Health Research Institute - University Hospital "Fundacion Jimenez Diaz", 28040 Madrid, Spain
[6]Lead Contact
*Correspondence: fatima.gebauer@crg.eu
http://dx.doi.org/10.1016/j.ccell.2016.10.004

SUMMARY

RNA binding proteins (RBPs) modulate cancer progression through poorly understood mechanisms. Here we show that the RBP UNR/CSDE1 is overexpressed in melanoma tumors and promotes invasion and metastasis. iCLIP sequencing, RNA sequencing, and ribosome profiling combined with in silico studies unveiled sets of pro-metastatic factors coordinately regulated by UNR as part of RNA regulons. In addition to RNA steady-state levels, UNR was found to control many of its targets at the level of translation elongation/termination. Key pro-oncogenic targets of UNR included *VIM* and *RAC1*, as validated by loss- and gain-of-function studies. Our results identify UNR as an oncogenic modulator of melanoma progression, unravel the underlying molecular mechanisms, and identify potential targets for this therapeutically challenging malignancy.

INTRODUCTION

Melanoma is an increasingly prevalent cancer that remains a paradigm of genetically and histopathologically heterogeneous diseases (Schadendorf et al., 2015). Both benign and malignant lesions can share dysplastic features that greatly complicate diagnosis. Despite great progress in dermoscopic techniques, staging is still largely defined on the basis of the thickness of the primary melanocytic lesion, although this criterion is long known to be subject to error (Thompson et al., 2004). Activating alterations in key signaling cascades (e.g., driven by BRAF or MEK) have resulted in the development of molecularly guided therapies, but response rates are frequently transient (Flaherty et al., 2012). Inhibitors of checkpoint blockers such as CTLA-4, PD1, or PDL1 are providing unprecedented durable responses, although only to a fraction of metastatic melanoma patients (Bathia and Thompson, 2016). Thus, the melanoma field is in need of diagnostic and prognostic biomarkers, as well as new targets for drug development.

High-throughput sequencing efforts have revealed massive heterogeneity of the melanoma transcriptome (Dutton-Regester and Hayward, 2012). Despite this defining property, RNA-related mechanisms remain surprisingly understudied. A comprehensive analysis of RNA binding proteins (RBPs) and their targets in the context of melanoma initiation and progression seems lacking. RBPs are particularly relevant because they can modulate every post-transcriptional step of gene expression, from splicing in the nucleus to mRNA export, localization, translation, or decay in the cytoplasm. Each single RBP can bind to hundreds of mRNAs, forming extensive networks in which

Significance

RNA binding proteins (RBPs) are gaining great attention in cancer research for their potential to regulate essentially every hallmark of tumor development. Yet the molecular mechanisms that underlie these capacities are unclear, particularly in aggressive cancers such as melanoma, where RBPs remain largely uncharacterized. Our work establishes that the RBP UNR/CSDE1 is a critical modulator of melanoma metastasis, and reveals a network of UNR targets including well-known cancer drivers as well as genes not previously linked to the disease. Our data broaden the functions of UNR, unveiling a role in translation elongation/termination, and highlight the physiological relevance of RBP-mediated control of oncogenic networks in cancer.

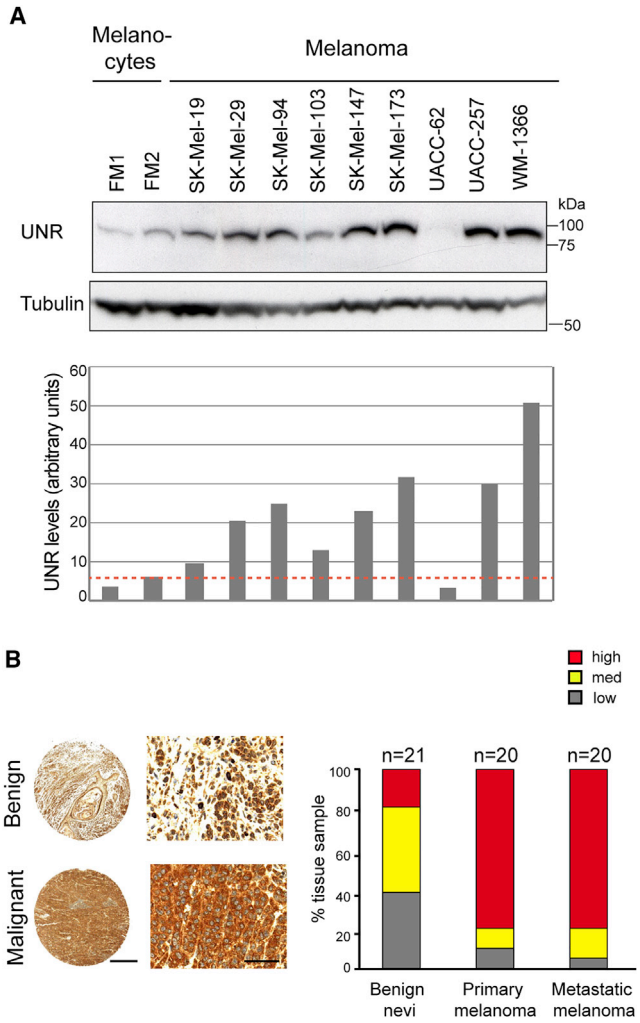

Figure 1. UNR Is Upregulated in Melanoma

(A) Western blot of UNR in melanoma cell lines and non-tumoral melanocytes. Tubulin is shown as a loading control. A quantification of the UNR signal corrected for tubulin is shown at the bottom. A red dashed line has been drawn at the levels observed in melanocytes to facilitate inspection.

(B) UNR expression in malignant and benign patient tumor samples monitored by immunohistochemistry (IHC). The same commercial anti-UNR antibody used in (A) was employed for IHC. IHC scoring was performed blind, prior to association with clinical data. Left and right scale bars represent 200 μm and 20 μm, respectively.

See also Figure S1.

functionally related genes may be co-regulated, representing "RNA regulons" (Morris et al., 2010). As a result, RBP malfunction may have dramatic consequences for cell physiology. Indeed, RBPs are emerging as critical modulators of cancerous traits, yet little is known about the underlying mechanisms and key downstream targets (Wurth and Gebauer, 2015).

Upstream-of-N-Ras (UNR), known as CSDE1 in mammals, is a conserved RBP containing five cold-shock domains (CSDs) that bind single-stranded RNA (Goroncy et al., 2010; Triqueneaux et al., 1999). UNR locates primarily in the cytoplasm, where it regulates mRNA translation and stability (reviewed in Mihailovich et al., 2010). In *Drosophila*, UNR inhibits cap-dependent translation of *msl-2* mRNA and modifies the structure of *roX2* long non-coding RNA, both events contributing to the regulation of X chromosome dosage compensation (Abaza et al., 2006; Duncan et al., 2006; Militti et al., 2014). In the case of *msl-2*, UNR binds to the 3′ UTR together with the RBP SXL, establishing extensive intertwined interactions that explain cooperative RNA recognition (Hennig et al., 2014). In the case of *roX2*, UNR can bind on its own. Thus, UNR binding requirements and regulatory mechanisms may vary depending on the target transcript. The versatile binding of UNR to RNA likely underlies the diverse biological roles of this protein. In mammals, UNR may either promote or inhibit apoptosis and differentiation depending on cell type (Dormoy-Raclet et al., 2007; Elatmani et al., 2011; Horos et al., 2012).

RNA immunoprecipitation (RIP) analysis revealed that *Drosophila* UNR binds to hundreds of transcripts (Mihailovic et al., 2012). Among these, mRNAs encoding conserved regulators related to human cancer progression were identified (e.g., *TGFB1*, *ABL1*, or *CTNNB1*). The targets of mammalian UNR have not been described at genome-wide level. However, the small list of known targets suggests a potential role of UNR in proliferation and cancer progression. For example, UNR participates in the destabilization of *FOS* mRNA by binding to its coding sequence (CDS) (Chang et al., 2004). In addition, UNR regulates internal ribosome entry site (IRES)-dependent translation of the transcripts encoding the oncogene MYC, the cell-cycle kinase PITSLRE, and the apoptosis regulator APAF-1 (Evans et al., 2003; Mitchell et al., 2003; Tinton et al., 2005). Furthermore, UNR represses the translation from its own IRES, providing a negative feedback loop to temper the levels of UNR along the cell cycle (Schepens et al., 2007).

Here, we have evaluated the potential role of UNR in cancer progression using melanoma as a model system.

RESULTS

UNR Promotes Melanoma Cell Invasion and Metastasis

To obtain insights into a potential role of UNR in cancer progression, we first interrogated the TCGA database for alterations of *CSDE1/UNR* expression in a variety of human cancer samples. *CSDE1* mRNA is upregulated in a high percentage of tumors, especially in skin and ovary cancers (Figure S1). We therefore focused on melanoma as a prototypical skin cancer. Because UNR negatively regulates its own translation (Schepens et al., 2007), RNA levels may not correlate with protein amounts. Hence, we monitored the levels of UNR protein in melanoma cell lines and tissue specimens. We found that UNR was overexpressed in a variety of melanoma cell lines compared with normal melanocytes. Importantly, we also observed high expression of UNR in primary and metastatic lesions from melanoma patients compared with benign nevi (Figures 1A and 1B).

An inducible short hairpin RNA (shRNA) system was then used to conditionally deplete UNR from a representative melanoma cell line (SK-Mel-103) characterized by its aggressive and metastatic properties (Figure 2A, left panel). A cumulative growth assay, which monitors proliferation in a confluence-independent manner, showed no differences between control and UNR-depleted cells (Figure 2A, middle panel). However, a reduction in cell number was observed when cells reached confluence

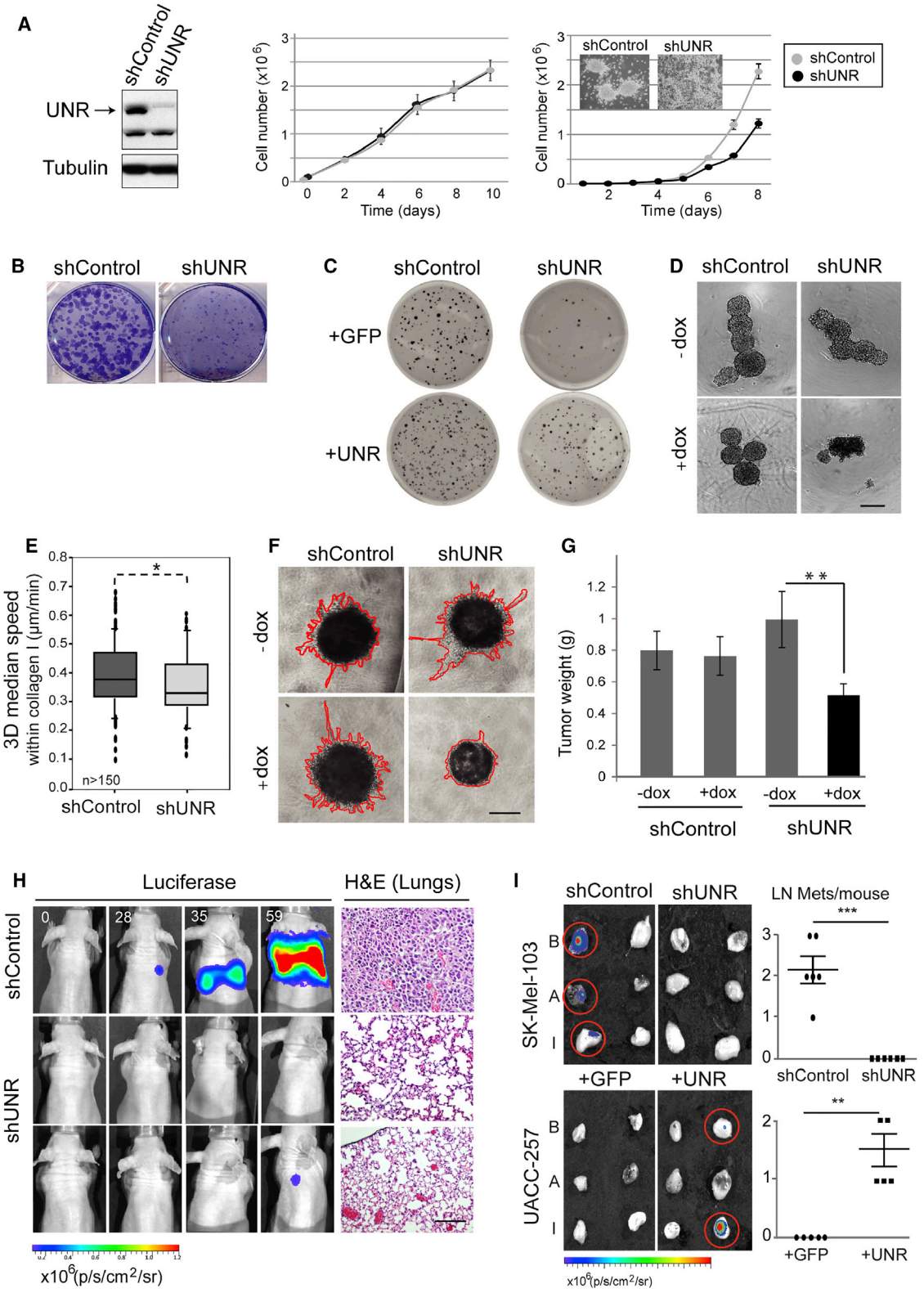

Figure 2. UNR Promotes Melanoma Invasion and Metastasis

(A) SK-Mel-103 melanoma cells were stably transduced with a lentiviral doxycycline inducible shRNA. Western blot (left), cumulative (middle), and standard (right) growth curves. Gray, shControl; black, shUNR. Error bars represent the SEM of triplicate experiments. The insets show typical bright-field microscopy views of shControl and shUNR cells.

(legend continued on next page)

(Figures 2A [right panel] and S2A). Furthermore, while control cells were able to grow as spheres, UNR-depleted cells remained tightly attached to the surface (Figure 2A, insets in right panel). These results suggest that UNR influences proliferation under stress conditions such as crowding. UNR depletion reduced the clonogenic capacity of melanoma cells and their ability to grow in soft agar (Figures 2B and 2C), results that were recapitulated in different melanoma cell lines characterized by prototypical genetic mutations (Figure S2B). Unless otherwise indicated, we henceforth used SK-Mel-103 cells. Restoring the expression of UNR in depleted cells using a cDNA resistant to shRNA inhibition rescued colony formation in soft agar, indicating that impaired colony formation upon UNR depletion is unlikely to result from off-target effects of the shRNA (Figures 2C and S2C). In addition, enforced expression of UNR in cancerous cells increased colony formation, suggesting that the dosage of UNR is important for colony growth (Figure S2C, right panel). These results suggest that UNR promotes anchorage-independent growth. This was further confirmed by growing cells in suspension. Contrary to control cells, UNR-depleted cells were unable to grow detached from the surface and underwent cell death as measured by caspase-3/7 cleavage activity (Figures 2D, S2D, and S2E), suggesting that UNR promotes resistance to anoikis. In addition, UNR depletion resulted in decreased migration of cells within collagen (Figure 2E).

Anchorage-independent growth, migration, and resistance to anoikis are frequently associated with invasive and metastatic capacities of tumor cells. To evaluate these properties more directly, we cultured melanoma spheroids in Matrigel and measured their invasion index. UNR-depleted cells formed significantly smaller spheroids with dramatically reduced invasion index (Figures 2F and S2F). To investigate how general these effects were, we depleted UNR in a number of melanoma cell lines and cells from other tumor origins (breast and ovarian cancer), carrying either wild-type or mutated *BRAF*, a gene frequently mutated in melanoma. In all cases, depletion of UNR favored anoikis and reduced the invasive capacities of cells (Figure S2H). Conversely, overexpression of UNR augmented these traits (Figure S2H). These results indicate that UNR promotes tumorigenesis in vitro.

Next, we validated the pro-tumorigenic functions of UNR in vivo, using xenograft models in mice. To this end, UNR-depleted SK-Mel-103 melanoma cells were implanted subcutaneously in immunodeficient mice. As shown in Figure 2G, UNR-depleted cells resulted in smaller tumors compared with control cells. To assess for UNR roles in surrogate models of metastasis, we labeled control and UNR-depleted cells with luciferase to monitor tumor growth and dissemination upon tail-vein injection. The results showed a striking reduction of the metastatic capacity of UNR-depleted cells to the lung, a frequent site for melanoma metastasis in mice (Figure 2H). For a more direct assessment of metastatic potential, mice were injected subcutaneously, and lymph nodes proximal and distal to the site of injection were monitored for the presence of tumor cells. Depletion of UNR from highly metastatic SK-Mel-103 cells indeed eliminated lymph node metastasis (Figure 2I). Conversely, overexpression of UNR in otherwise non-metastatic UACC-257 cells promoted migration and invasion in vitro, as well as lymph node metastasis formation in vivo (Figures 2I and S2G). Taken together, these data indicate that UNR is required to sustain the invasive and metastatic capacity of melanoma cells.

Identification of UNR Targets by iCLIP-Seq

To unravel the mechanisms by which UNR promotes invasion and metastasis, we intersected three types of high-throughput analysis: (1) individual-nucleotide resolution crosslinking immunoprecipitation sequencing (iCLIP-seq) to identify direct RNA targets of UNR, (2) RNA sequencing (RNA-seq), and (3) ribosome profiling to determine at which level UNR regulates the expression of its targets (Figure 3A).

To perform iCLIP-seq (Konig et al., 2011), we generated an anti-UNR antibody that immunoprecipitates endogenous UNR efficiently and with high specificity (Figure 3B [left panel] and Figure S3A). After UV crosslink of melanoma cells and partial RNA digestion, UNR-RNA complexes were immunoprecipitated and appeared as a smear over the UNR band in a protein gel (Figure 3B, right panel, red square). No complex was present in

(B) Colony-formation assay in cells as shown in (A). One representative whole well from a 6-well plate is shown per condition (n = 6).
(C) Soft agar assays of cells expressing shUNR or shControl, and GFP- or RNAi-resistant UNR-FLAG. One representative whole well from a 12-well plate is shown per condition (n = 10).
(D) Analysis of anoikis. Cells were grown in ultra-low attachment plates and growth was documented by bright-field microscopy. Scale bar represents 500 μm (n = 4).
(E) The mean speed of migration of SK-Mel-103 cells embedded into collagen was analyzed by time-lapse microscopy. The number of cells analyzed from three different experiments is indicated (n). Center lines show the medians, box limits indicate the 25th and 75th percentiles as determined by R software, whiskers extend 1.5 times the interquartile range from the 25th and 75th percentiles, and outliers are represented by dots.
(F) Invasion assay of cell spheres embedded in Matrigel monitored by bright-field microscopy. The invasion area is shown in red (n = 4). Scale bar represents 500 μm.
(G) shControl or shUNR cells were injected subcutaneously into nude mice. Tumors were resected and weighed (n = 18 shControl, n = 16 shControl + dox, n = 18 shUNR, n = 19 shUNR + dox). Error bars represent SEM.
(H) Melanoma shUNR and shControl cells expressing a luciferase reporter were injected into the tail vein of nude mice and metastasis to the lung was followed (n = 5 mice per experimental genotype). Lung architecture was analyzed by H&E staining. Scale bar represents 50 μm.
(I) Metastatic SK-Mel-103 cells expressing shUNR or shControl (upper panel, n = 6) or non-metastatic UACC-257 cells expressing UNR or control GFP (lower panel, n = 5) were injected subcutaneously into the flanks of nude mice. All cells contained a luciferase reporter. Tumors were allowed to grow until they reached 1,500 mm^3, at which moment the sentinel (inguinal, I) and distal (axillary, A; brachial, B) lymph nodes at both sides of the animal were extracted and analyzed for the presence of metastatic cells. Representative images are shown at the left, where red circles mark positive lymph nodes for metastasis. A quantification is shown at the right. Center lines show the mean value and side bars represent 1 SD as calculated by GraphPad software. The number of lymph node metastases in each animal is represented by dots.
Significance was assessed by Student's t test (*$p \leq 0.05$, **$p \leq 0.01$, ***$p \leq 0.001$). See also Figure S2; Movies S1 and S2.

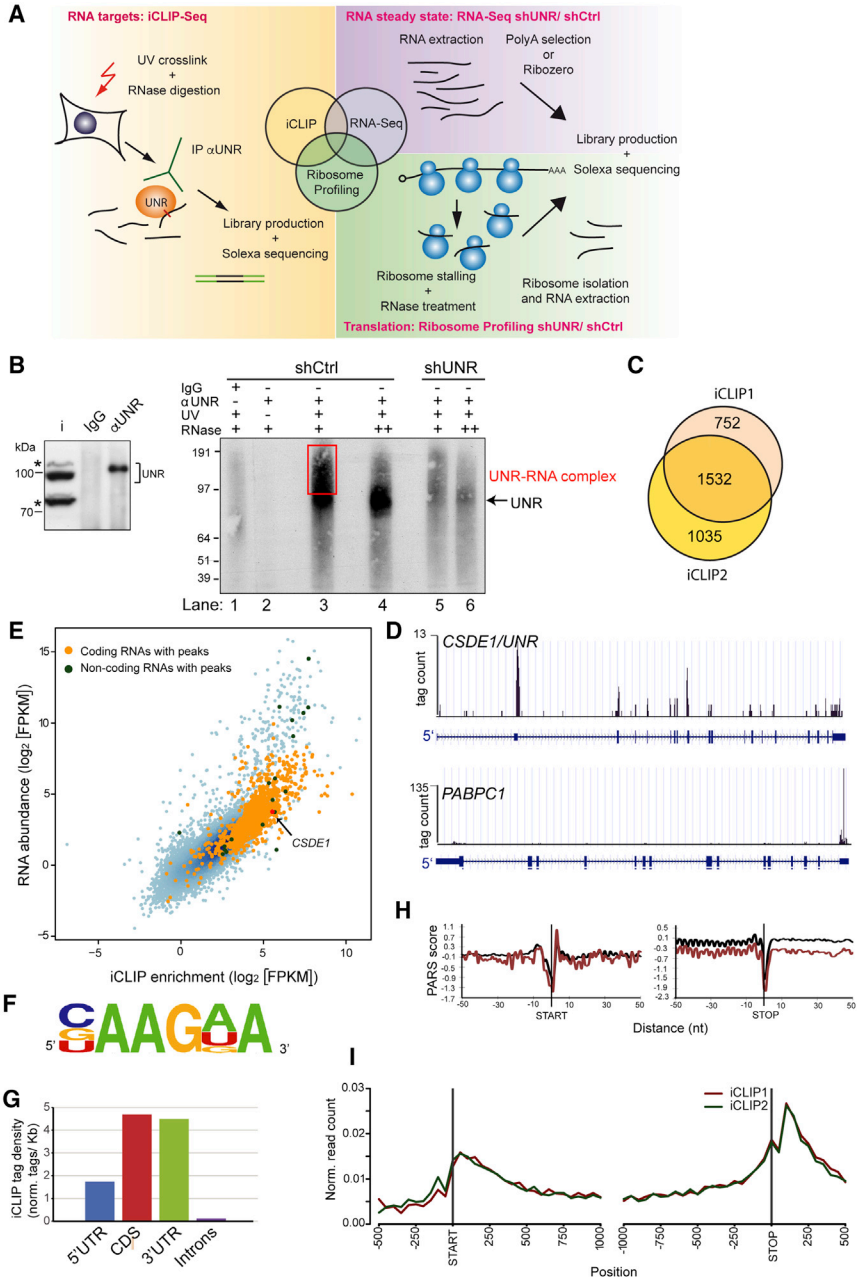

Figure 3. Identification of UNR RNA Targets by iCLIP-Seq

(A) Experimental strategy to unravel the molecular mechanisms underlying the role of UNR in melanoma.

(B) iCLIP controls. Left: western blot of anti-UNR (αUNR) and control (IgG) immunoprecipitates with our αUNR antibody; i, input. Asterisks denote non-specific bands. Right, UNR-RNA complexes used in iCLIP (see text for details).

(C) Venn diagram depicting the number of targets identified in two independent iCLIP experiments.

(D) UNR iCLIP profiles for *PABPC1* and *CSDE1/UNR* mRNAs.

(E) Scatter plot showing the correlation between UNR binding (iCLIP tag enrichment) and UNR target levels (mRNA abundance). Orange and green dots depict coding and non-coding RNAs with called UNR peaks, respectively. Blue dots depict RNAs with no detectable UNR binding.

(F) UNR binding motif.

(G) UNR iCLIP tag density in different transcript regions.

(H) PARS analysis of the structure of UNR targets (brown) compared with all transcripts (black).

(I) Metagene analysis of UNR binding along the mRNA. Tag counts are normalized for coverage within the experiment.

See also Figure S3; Tables S1, S2, S3, and S6.

control lanes lacking UV crosslinking or immunoprecipitated with rabbit immunoglobulin G (IgG), indicating specificity (Figure 3B, lanes 1 and 2). In addition, upon extensive digestion with RNase the signal of the complex was reduced to a sharp band close to the molecular weight of UNR (Figure 3B, lane 4) that was barely detectable in UNR-depleted cells (Figure 3B, lanes 5–6). We performed two independent iCLIP experiments that showed a high correlation (Figure S3B; see Table S1 for iCLIP statistics), revealing a set of 1,532 common targets (Figure 3C and Table S2). Most of these targets are protein-coding RNAs, while only few long-non-coding RNAs were identified. Strikingly, 18.5% of the common targets overlap with *Drosophila* UNR targets previously identified by RIP sequencing (Mihailovic et al., 2012), which is considerable given the strong divergence between the two species (Table S2), suggesting conserved functions for UNR. The vast majority of the remaining targets have not been previously described in the literature. Of the known targets of mammalian UNR, only *PABPC1* and *CSDE1* mRNAs were retrieved in our system. Binding of UNR to its own mRNA occurred preferentially at the 5′ UTR, consistent with the proposed role of UNR regulating translation from its own IRES (Schepens et al., 2007) (Figure 3D). However, unlike previous reports, binding to *PABPC1* mRNA was detected preferentially at the 3′ UTR (Figure 3D), suggesting potential additional regulatory mechanisms of this transcript (Patel et al., 2005). Identified UNR targets included a significant fraction of ribosomal protein and histone mRNAs, among others (Table S2). Gene ontology (GO) analysis showed enrichment for ER-associated translation, extracellular components, exosome, cell junctions, focal adhesions, or melanosome, which fit well with functions of UNR in invasion and metastasis (Figure S3C and Table S3). Interestingly, of the 1,532 UNR targets, 396 were found to be linked to cancer development (Table S2). Validation of a subset of these targets by independent RNA immunoprecipitation experiments showed an 89% validation rate (Figure S3D). Thus, a high proportion (26%) of UNR targets encodes cancer-related factors previously unknown to be regulated by this RBP.

UNR Binding Properties

iCLIP enrichment of UNR targets showed a general correlation with RNA abundance, suggesting relaxed sequence binding requirements for this protein (Figure 3E). Binding is nevertheless specific, as many highly abundant transcripts were not bound by UNR. DREME analysis identified a consensus binding motif similar to that described by in vitro SELEX experiments (Triqueneaux et al., 1999) (Figure 3F). UNR binds mature mRNA, preferentially in the CDS and the 3′ UTR and to a lesser extent in the 5′ UTR, suggesting functions for UNR in addition to its described roles as an IRES *trans*-acting factor (ITAF) (Figure 3G). Overall, the binding motif is centered around the UNR iCLIP peaks; however, when different regions of the mRNA are considered separately, a strong tendency for the motif to be located in the center of the iCLIP tags is detected for CDS peaks but not for 5′ or 3′ UTR peaks, suggesting different binding modes of UNR to these regions (Figure S3E). RNA structural analysis using experimental PARS (parallel analysis of RNA structure) data shows a drop in the PARS score at UNR peaks, indicating that UNR binds single-stranded RNA (Figure S3F) (Wan et al., 2014). In addition, UNR targets show significantly decreased PARS scores compared with all transcripts, indicating a preference of UNR for unstructured mRNAs (Figure 3H). Metagene analysis of the position of UNR binding along the mRNA shows preference of binding downstream of the start and/or stop codons, as well as at the stop codon (Figure 3I). This binding profile is specific for UNR, as we did not observe it for other RBPs such as HuR or TDP43 (Figure S3G).

UNR Regulates the Levels of Transcripts Encoding Oncogenes and Tumor Suppressors

Binding by an RBP does not necessarily imply regulation of the bound target at the tested condition. To identify iCLIP targets regulated by UNR, we first undertook RNA-seq analysis of cells where UNR had been depleted for 5 days compared with shControl pairs. To obtain complete information about coding and non-coding RNAs, we performed RNA-seq on both poly(A) RNA and total RNA after ribozero treatment, each in duplicate. The duplicates showed high correlation (Figure S4A; see also Table S1 for statistics). Because UNR binds mostly mature mRNAs, we focused our analysis on poly(A) RNA-seq. For histone mRNAs, which lack poly(A) tails, we used total RNA-seq.

Evaluation of iCLIP enrichment and RNA abundance changes showed a poor correlation, indicating that only a reduced number of binding targets were regulated by UNR at the steady-state level (Figure 4A). A total of 715 genes showed altered RNA levels, 93 of which were direct UNR targets (Figure 4B). Comparatively more mRNAs were downregulated upon UNR depletion, suggesting prevalent roles of UNR as an activator of mRNA accumulation (Figure 4B). GO analysis of regulated iCLIP targets (other than histones and ribosomal protein mRNAs) showed over-representation of cell adhesion and extracellular matrix components (Figures 4C and Table S4). We selected iCLIP targets encoding factors involved in these functions for validation and observed consistent downregulation of tumor-promoting factors upon UNR depletion, while tumor-suppressing factors were upregulated (Figure 4D). A transcript downregulated by UNR encodes the tumor suppressor PTEN, a gene whose expression is frequently reduced in melanoma. We find upregulation of PTEN both at the mRNA and protein levels upon UNR depletion (Figures 4D and S4B).

Finally, we tested whether the regulation of mRNA levels by UNR was associated with a specific binding pattern of UNR along the transcript. Interestingly, a meta-analysis indicated strong positioning of UNR at the stop codon of regulated transcripts (Figure 4E). mRNAs upregulated upon UNR depletion (i.e., downregulated by UNR) showed additional binding of UNR at the start codon.

In summary, UNR regulates the steady-state levels of mRNAs coding for tumor-promoting and -suppressing factors in a manner that correlates with its oncogenic properties.

UNR Regulates Critical Melanoma Genes at the Translation Level

Given that UNR binds to a subset of melanoma transcripts, we expected this protein to be an mRNA-specific regulator. To rule out indirect effects on global translation, we analyzed de novo protein synthesis by ^{35}S metabolic labeling as well as polysome profiling of shUNR versus shControl cells. We did not detect significant differences in global translation by any of these assays (Figure S5A).

To identify genes regulated by UNR at the translation level, we performed ribosome profiling (RP), a technology that provides quantitative and positional information of ribosomes along transcripts at codon resolution (Ingolia et al., 2009). Three independent RP experiments were performed on shUNR and shControl cells after a 5-day induction of the shRNA. These experiments showed a good correlation (Figure S5B). Metagene analysis indicated that reads mapped primarily at the CDS, ending abruptly at the stop codon and extending to some degree into the 5′ UTR, typical of RP. In addition, single-nucleotide resolution analysis revealed the triplet (codon) pace of the ribosome, attesting to the quality of our data (Figure S5C). Our coverage was nevertheless limited, as lowly abundant genes could not be quantified with statistical significance (see Table S1). For example, β-catenin (*CTNNB1*) mRNA appears as "not translationally regulated" by our statistical analysis. However, western blot analysis showed that the levels of CTNNB1 decrease upon UNR depletion even in the presence of proteasome inhibitors, suggesting that UNR promotes *CTNNB1* translation (Figure S5D, left panel).

The details of our RP analysis are described in Supplemental Experimental Procedures (see also Figure S5E). In brief, we performed three types of analyses: (1) we considered all transcripts and normalized the number of ribosome protected fragments (RPFs) with their RNA levels (translational efficiency or "TE" group); (2) we excluded transcripts changing at the steady-state level and quantified normalized RPFs ("RPF" group); and (3) we analyzed the distribution of ribosomes along the mRNA, even for transcripts that did not change at the TE or RPF levels ("Distribution" group). Altogether, the analysis revealed 451 genes regulated at the translation level, of which 127 are UNR iCLIP targets (Figure 5A; Tables S5 and S6). GO analysis of UNR targets (excluding histone and ribosomal protein mRNAs) showed enrichment in categories related to the extracellular matrix, among others (Figure 5B and Table S5).

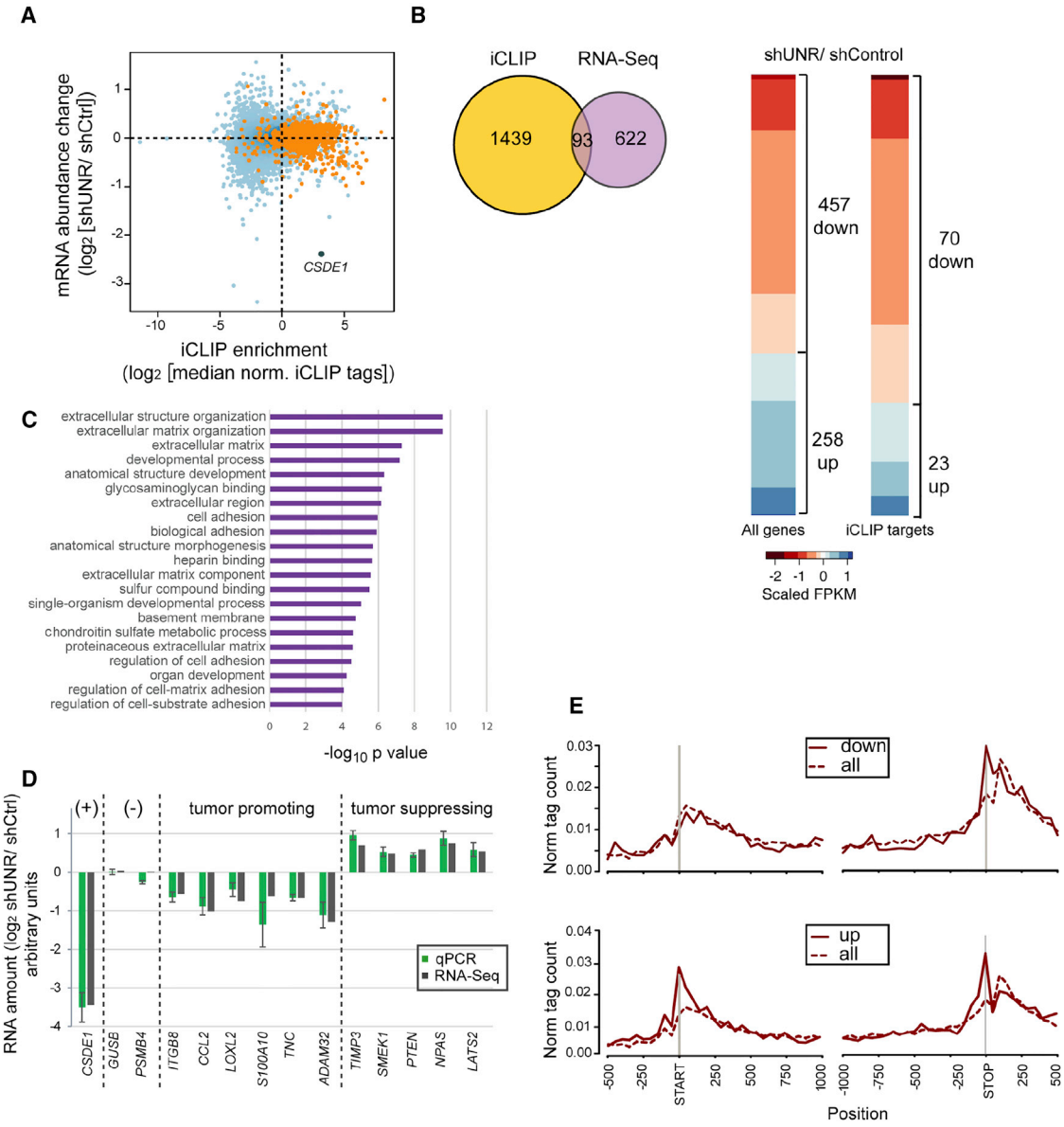

Figure 4. UNR Targets Regulated at the Steady-State Level

(A) Scatter plot showing the correlation between iCLIP tag enrichment and mRNA abundance change between shUNR and shControl cells. Orange points denote UNR targets.

(B) Left: Venn diagram illustrating the overlap of genes regulated at the steady-state level and iCLIP targets. Right: Heatmaps of changes in RNA levels upon UNR depletion for all genes and iCLIP targets.

(C) GO analysis of all genes changing at the steady-state level. Similar results were obtained for iCLIP targets.

(D) Validation of transcript level changes by qRT-PCR. *GUSB* and *PSMB4* were used as negative controls. RNA-seq data are included as comparison. Error bars represent SEM of at least three experiments.

(E) Metagene analysis of UNR binding in regulated transcripts.

See also Figure S4; Tables S1, S4, and S6.

A summary of all changes observed upon UNR depletion is shown in Figure 5C. In this graph, mRNA abundance change is plotted against changes in the number of RPFs. Quadrants a and c are the most populated, and show genes for which there is a positive correlation between mRNA abundance and translation, while almost no changes are detected in the anti-correlation quadrants d and b. These results nicely illustrate that our RP data reproduce events observed at the RNA-seq level. However, most UNR direct targets (orange crosses) fall outside these quadrants and are present in the green, pink, and white areas. The green regions represent genes that change at the mRNA steady-state level without significant differences in RPF reads. Transcripts in these regions show differences in amount that are not reflected at the level of ribosome association and,

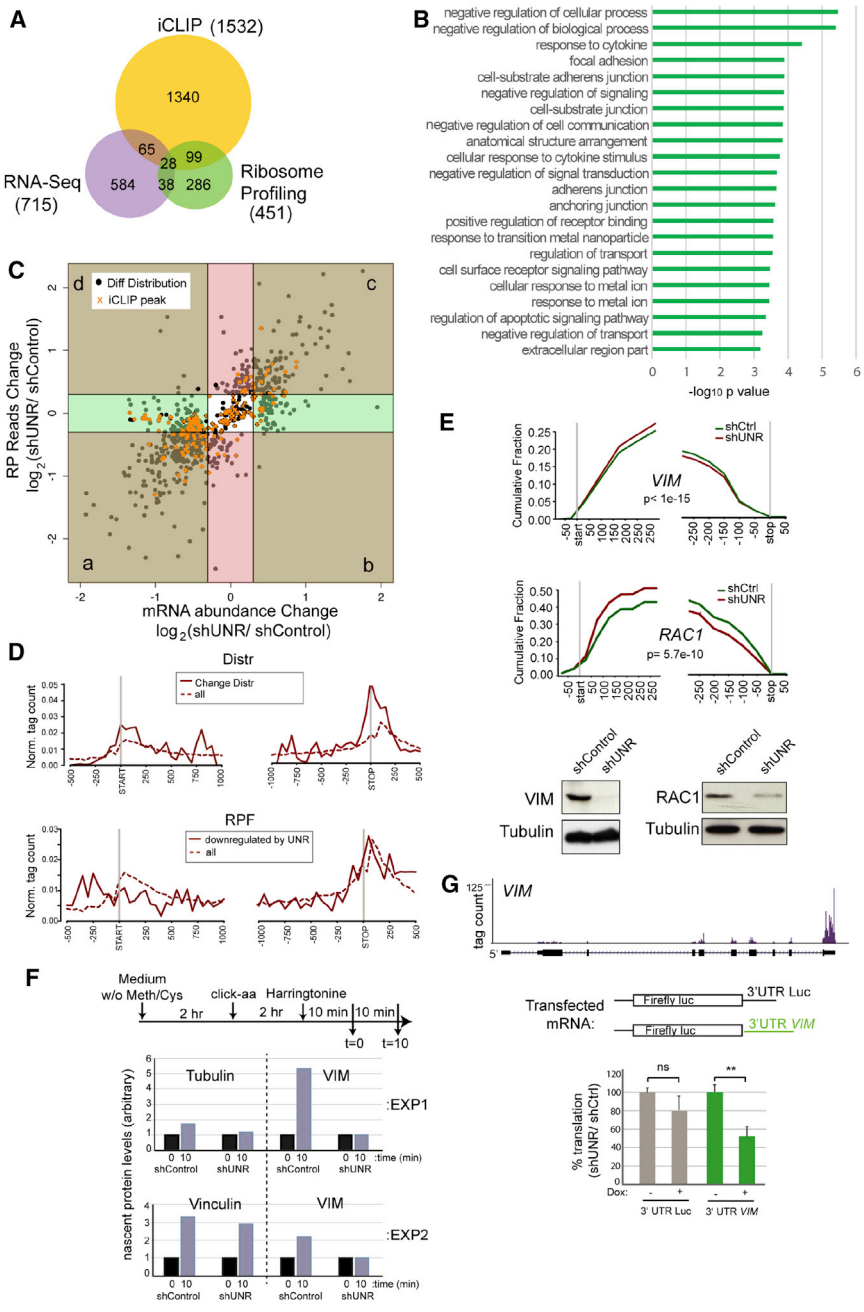

Figure 5. UNR Targets Regulated at the Translation Level

(A) Venn diagram depicting the overlaps of the analysis performed in this study.

(B) GO analysis of genes changing at the translation level upon UNR depletion. Similar results were obtained for direct UNR targets.

(C) Summary of all changes detected upon UNR depletion (see text for details). Black, mRNAs showing ribosome distribution changes; orange, UNR targets.

(D) Metagene analysis of UNR position along the mRNA in transcripts regulated at the level of ribosome distribution or RPF.

(E) Top: ribosome distribution changes on *VIM* and *RAC1* mRNAs upon UNR depletion; p values for the significance of differences in distribution are shown (Smirnov-Kolmogorov, two-sample, two-sided test). Bottom: effect of UNR depletion on VIM and RAC1 protein levels.

(F) Ribosome run-off assays. Newly synthesized VIM, tubulin, and vinculin were monitored in shControl and shUNR cells by metabolic labeling using amino acids susceptible to click chemistry. A scheme of the labeling protocol is shown at the top. Translation initiation was inhibited with Harringtonine for 10 min, and samples were taken at 0 or 10 min after Harringtonine inhibition. Newly synthesized proteins were labeled with biotin using click chemistry, selected with streptavidin beads, and resolved by SDS-PAGE followed by western blot. Proteins were quantified and plotted relative to the levels at t = 0. Two independent experiments (EXP1 and EXP2) were performed.

(G) Top: iCLIP profile of UNR binding to *VIM* mRNA. Bottom: firefly luciferase reporter mRNAs were transfected into shControl and shUNR melanoma cells treated or not with doxycycline. Luciferase values were corrected for luciferase mRNA levels, and represented as the efficiency of translation relative to shControl cells.

Error bars represent SEM of triplicate experiments. Significance was assessed by Student's t test (ns, not significant; **p = 0.0005). See also Figure S5; Tables S1, S5, and S6.

therefore, these transcripts are translationally compensated. A significant proportion of UNR targets fall in these areas, most of which correspond to histone mRNAs.

The pink areas show genes that do not change at the mRNA level but at the RPF level. We anticipate that these genes are regulated at the level of translation initiation, which results in changes in the number of ribosomes associated to the mRNA. As UNR has been shown to regulate translation initiation, we expected most of the UNR iCLIP targets to appear in these areas. Surprisingly, however, this is not the case. As shown in Figure 5C, multiple genes do not change either at the mRNA or RPF levels (middle white square). Interestingly, these genes display changes in the relative distribution of ribosomes along the CDS (black dots). Most of these transcripts are direct UNR targets (orange crosses). Altogether, of the 127 direct UNR targets regulated at the translation level, 20 (16%) show changes only in RPF levels while 60 (47%) display changes only in ribosome distribution (Table S5). Changes in ribosome distribution without accompanying changes in RPF levels likely reflect regulation at the translation elongation or termination steps. Thus, these results suggest that, unexpectedly in comparison with previous literature, UNR regulates translation of its melanoma targets mainly at the level of elongation or termination. Consistently, in addition to subpolysomal fractions, UNR was found to be associated to early translating ribosomes in sucrose gradients (Figure S5F).

Similar to transcripts regulated at the steady-state level (Figure 4), examination of the UNR binding profile in transcripts showing differential ribosome distribution revealed a stronger

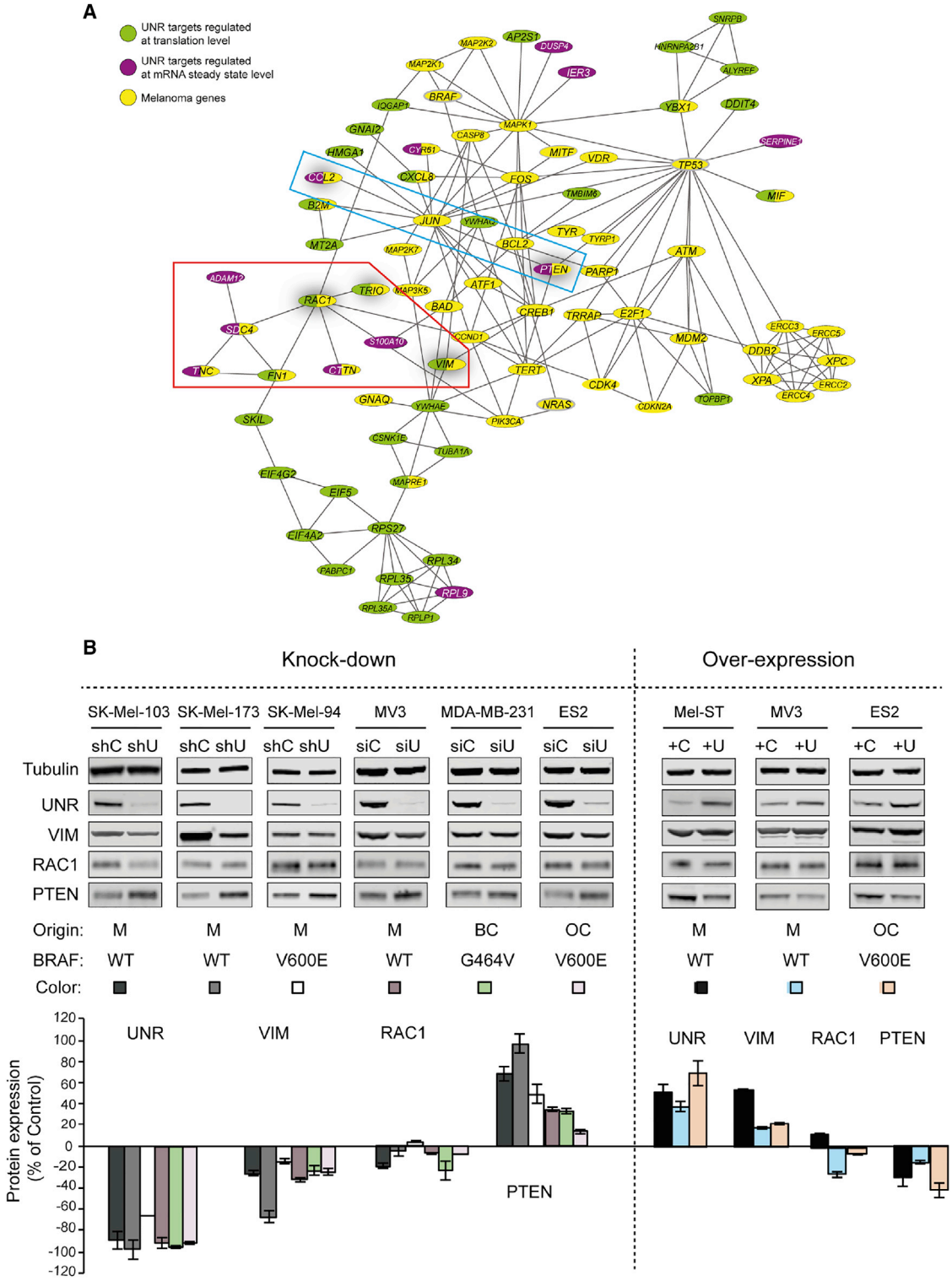

Figure 6. UNR Regulates a Network of Genes Relevant for Melanoma Progression

(A) Network analysis of UNR targets. Yellow, melanoma-relevant genes. Targets regulated by UNR at the steady-state (violet) or translation (green) levels that intersect with melanoma genes are shown. Connections represent interactions, broadly defined as metabolic catalysis, co-regulation, protein interaction, same complex, reaction with, and state change (i.e., post-translational modification or change in subcellular localization). Boxes enclose RNA regulons discussed in the text. Genes studied in more detail in this report are shadowed.

(legend continued on next page)

positioning around the start and/or stop codons (Figure 5D). In addition, transcripts downregulated by UNR at the RPF level showed a shift of UNR binding toward the 5′ UTR.

To validate our RP analysis we first selected *TRIO*, a gene encoding a Rho guanine nucleotide exchange factor (GEF) involved in uveal melanoma (Vaqué et al., 2013). *TRIO* is a direct UNR target that shows reduced RPF levels upon UNR depletion without accompanying changes at the RNA level, suggesting decreased translation initiation (Table S5). Indeed, western blot analysis confirmed downregulation of TRIO protein in UNR-depleted cells (Figure S5G). We further focused on two genes that are highly altered in malignant melanoma, *VIM* (Vimentin) and *RAC1* (Ras-related C3 botulinum toxin substrate 1). VIM is a component of intermediate filaments that furnishes cells with resilience to changes in shape and is a marker of epithelial-to-mesenchymal transition (EMT), while RAC1 is a guanosine triphosphatase (GTPase) belonging to the Ras superfamily with pleiotropic effects. Both proteins are important for invasion and metastasis (Bid et al., 2013; Satelli and Li, 2011). *VIM* and *RAC1* are regulated at the level of ribosome distribution, with no changes in RNA amounts or crude RPFs (Table S5). Analysis of RP data indicated a redistribution of ribosomes toward the 5′ end in UNR-depleted cells for both transcripts, suggesting that they are translationally stimulated by UNR at the level of elongation (Figure 5E). Indeed, western blot analyses revealed a strong downregulation of these proteins in UNR-depleted cells (Figure 5E). Downregulation of VIM and RAC1 in the absence of UNR persisted in the presence of proteasome inhibitors, indicating a role for UNR in synthesis and not stability of these proteins (Figure S5D, middle and right panels). To confirm regulation after translation initiation, we performed ribosome run-off assays using metabolic labeling. Newly synthesized VIM was monitored for 10 min after inhibition of translation initiation with Harringtonine. In these conditions, synthesis of VIM was strongly downregulated in UNR-depleted cells, while synthesis of tubulin and vinculin was marginally affected (Figure 5F). To investigate the mechanism further, we performed reporter assays. Our iCLIP data indicate that UNR binds primarily to the 3′ UTR of *VIM* mRNA (Figure 5G). Transfection assays with mRNA reporters containing or lacking *VIM* 3′ UTR confirmed that UNR upregulates *VIM* at the level of translation by binding to the 3′ UTR (Figure 5G).

In conclusion, RP provides a list of cancer-relevant genes regulated by UNR at the level of translation, including critical melanoma genes. In addition, the data identify a role of UNR in translation elongation/termination.

Regulation of *VIM* and *RAC1* mRNA Translation by UNR Promotes Cancerous Traits

To identify candidate downstream effectors of UNR in melanoma progression, we performed network analyses. We retrieved melanoma-relevant genes from the MelGene (Athanasiadis et al., 2014), Cosmic Cancer Gene Census (Futreal et al., 2004), and KEGG CANCER (Kanehisa and Goto, 2000; Kanehisa et al., 2014) databases, in addition to individual publications (see Supplemental Information for a complete list of references) and constructed a curated list of 74 "melanoma genes." These genes are highly mutated in melanoma and/or are reported to control tumorigenic features of melanoma cells (Table S7). This list was intersected with UNR-regulated iCLIP targets to build a network with interaction data from Pathway Commons (Cerami et al., 2011) using the Cytoscape 3.1.1 platform (Shannon et al., 2003). The interactions include physical interactions (including co-occurrence in a complex), co-regulation, and molecular modification.

Strikingly, 66% of the melanoma genes are connected directly or indirectly with UNR targets (Figure 6A). Among these targets we find 15 genes that are also "melanoma genes" (*VIM*, *RAC1*, *PTEN*, *B2M*, *CCL2*, *CTTN*, *CXCL8*, *CYR61*, *FN1*, *MAPRE1*, *MIF*, *SDC4*, *TNC*, *TRIO*, and *YBX1*). Thus, 15 out of 45 UNR targets in the network have a direct implication in melanoma. Other targets are involved in cancer progression but currently unknown to play a role in melanoma (*HNRNPA2B1*, *IER3*, *GNAI2*, *HMGA1*, *YWHAQ*, *YWHAE*, *ADAM12*, *EIF4A2*, *PABPC1*, and *EIF4G2*) while the remaining targets have not been previously related to cancer progression. These results highlight the potential of UNR to influence multiple aspects of melanoma biology, as well as the potential of the network to uncover activities involved in melanoma progression. Among the targets, we find coherent sets of activities influencing melanoma cell survival, invasion, and metastasis (Figure 6A, blue and red boxes), identifying post-transcriptional regulons coordinated by UNR in melanoma development (see Discussion).

To assess the relevance of selected UNR targets in melanoma progression, we first checked whether their levels changed according to their expected regulation by UNR in the same set of cells previously scored for anoikis resistance and invasion. We found that UNR depletion reduced the levels of VIM and RAC1 in most cells while it increased the levels of PTEN (Figure 6B). Conversely, mild overexpression of UNR increased VIM and decreased PTEN levels, while the effect on RAC1 was more variable (Figure 6B). Taken together, these results indicate that the levels of VIM, RAC1, and PTEN are consistently regulated by UNR across a panel of cell lines. To assess whether translational regulation by UNR was relevant for melanoma progression, we tested whether overexpression of the translational targets *VIM* and *RAC1* could overcome the defects in anchorage-independent growth resulting from UNR depletion. As control we selected *LOXL2*, a gene involved in cancer cell invasion and also regulated by UNR (Figure 4D), but not present in the network (Figure 6A). As expected, depletion of UNR dramatically reduced the number and size of colonies that grow in soft agar (e.g., Figure 7A). While LOXL2 overexpression did not show a significant effect (Figure 7A), VIM and RAC1 overexpression fully restored colony growth and number (Figure 7B). These results indicate that regulation of *VIM* and *RAC1* mRNA translation by UNR contributes to melanoma traits. Furthermore, the results validate the

(B) UNR was either depleted or overexpressed and the levels of protein products were analyzed by western blot. Depletion of UNR was induced by shRNA expression (shU) or by transfecting small interfering RNA (siRNA) pools (siU) for 72 hr. Non-specific shRNA (shC) or siRNA pools (siC) were used as controls. Overexpression was achieved using viral expression constructs containing UNR (+U) or GFP (+C) as control. Quantifications from three independent experiments is shown at the bottom. Error bars represent SD. M, melanoma; BC, breast cancer; OC, ovarian cancer.

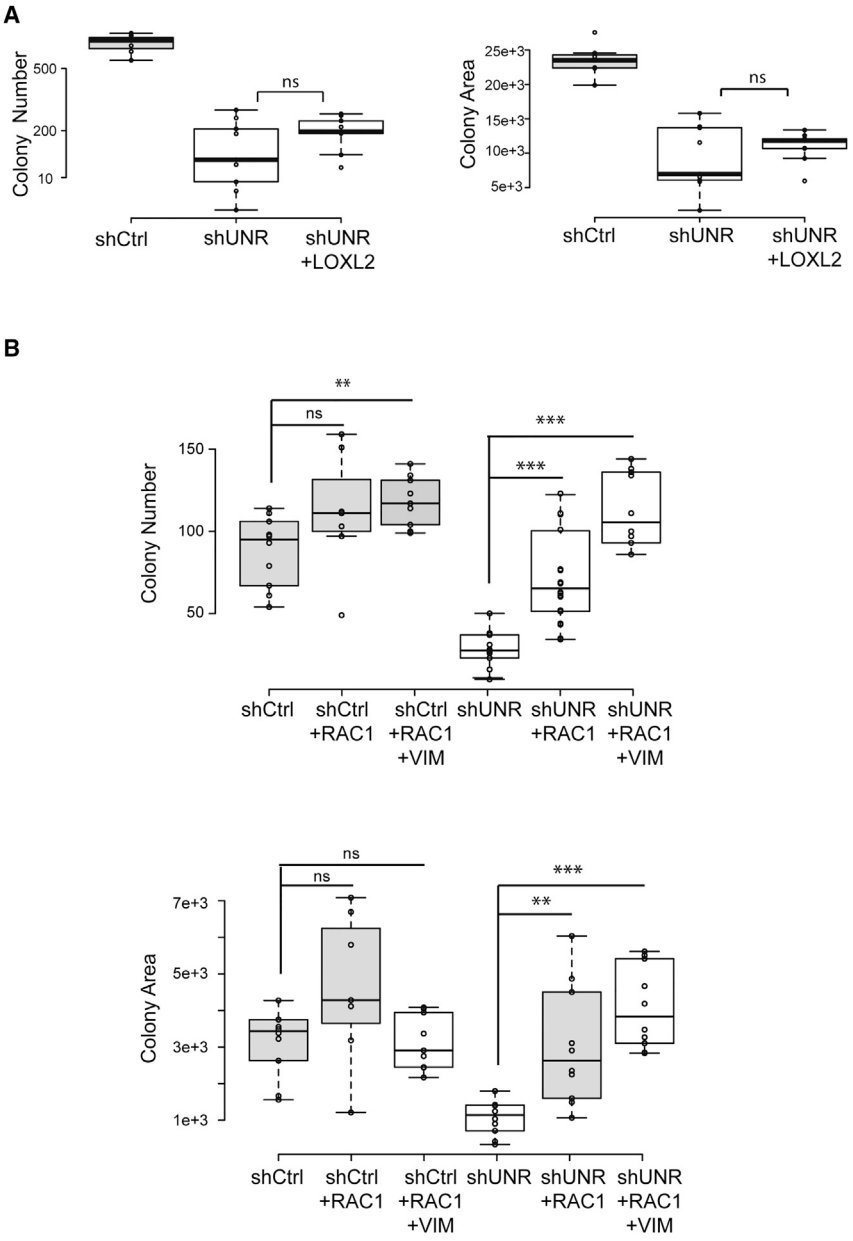

Figure 7. Regulation of VIM and RAC1 by UNR Modulates Cancerous Traits

(A) Colony-forming capacity of UNR-depleted cells after overexpression of LOXL2 (n = 10).

(B) Colony-forming capacity of UNR-depleted cells after overexpression of VIM and RAC1 (n = 7–10). Box plots are defined as in the legend of Figure 2E. Significance was verified by Student's t test (ns, not significant; $^{**}p \leq 0.01$, $^{***}p \leq 0.001$). Colony number: shCtrl versus shCtrl + Rac1 + Vim, p = 0.0017; shUNR versus shUNR + RAC1, p = 8.3E−04; shUNR versus shUNR + RAC1 + VIM, p = 5.08E−05. Colony area: shUNR versus shUNR + RAC1, p = 0.0022; shUNR versus shUNR + RAC1 + VIM, p = 1.17E−06. See also Table S7.

potential of the network to uncover activities involved in melanoma progression.

DISCUSSION

RBPs are fundamental players in RNA metabolism, but their contributions to disease are only starting to be recognized (Castello et al., 2013; Darnell, 2010; Wurth and Gebauer, 2015). Here we show that the RBP UNR plays key roles in melanoma progression, identify relevant mRNA targets, and investigate the underlying mechanisms.

Perhaps the most unanticipated role of UNR found in this study is primarily related to melanoma invasion and metastasis, as shown in xenograft models in mice. Consistent with these results, our data indicate that UNR promotes anoikis resistance, migration, and invasion in cultured melanoma cells. Most strikingly, overexpression of UNR alone converted a non-metastatic melanoma cell into a metastatic one. In agreement with this, genome-wide and functional analyses revealed that UNR regulates a series of targets with GO terms enriched in extracellular matrix and cell adhesion components. Binding of UNR to its targets follows a particular pattern, with strong UNR positioning closely downstream of the start and/or stop codons. This binding pattern prevails even after removing abundant classes of transcripts that are bound by UNR, such as ribosomal protein or histone mRNAs. Although the significance of this positioning is currently unclear, it seems specific for UNR, because other well-known post-transcriptional regulators (HuR and TDP43) do not show the same binding pattern. Interestingly, binding of UNR shifts precisely to the start and/or the stop codons in regulated transcripts, suggesting that regulation by UNR is associated with recognition of these defining landmarks of the CDS.

A group of targets regulated by UNR en masse at the mRNA and translation levels encode histones. While histone mRNAs are downregulated upon UNR depletion, this is compensated for by an increase in their translational efficiency. Compensatory mechanisms seem to be commonplace when UNR perturbations are introduced in the cell, warning of the need for careful validation of endogenous protein levels when either mRNA amounts or translational efficiencies are considered in isolation. In addition, most transcripts showing changes are not direct UNR targets, indicating considerable secondary effects.

Our unbiased analysis revealed targets regulated by UNR at the level of translation initiation, consistent with the location of bulk UNR in non-polysomal fractions. A selective group of these shows preferential UNR binding at the 5′ UTR. Given the reported role of UNR as an ITAF (Evans et al., 2003; Mitchell et al., 2003; Schepens et al., 2007; Tinton et al., 2005), these

transcripts may represent targets containing undefined IRESs which may impact on melanoma progression. Nevertheless, the largest group of translationally regulated transcripts seems to be controlled after the initiation step. The accumulation of ribosomes at the 5′ of the CDS of many of these targets in the absence of UNR, and the fact that UNR associates with the first few polysomal fractions in sucrose gradients, suggest a role for UNR in early elongation.

Although most reports on translational regulation have focused on initiation (reviewed in Sonenberg and Hinnebusch, 2009), regulation of translation elongation is emerging as a mechanism that is important in situations of proteotoxic stress or heat shock (Liu et al., 2013; Shalgi et al., 2013). Few RBPs with roles in translation elongation have been reported. These include FMRP, hnRNP E1, and the PUF-AGO complex, all of which inhibit elongation by various mechanisms (Darnell et al., 2011; Friend et al., 2012; Hussey et al., 2011). For example, hnRNP E1 and the PUF-AGO complex bind to the 3′ UTR of target transcripts and interfere with the elongation factor eEF1A1 to prevent its release from the ribosome or block its GTPase activity, respectively. The hnRNP E1 mechanism is especially relevant for breast cancer progression, as transforming growth factor β-promoted phosphorylation of hnRNP E1 results in translation derepression and contributes to EMT (Hussey et al., 2011). Remarkably, our results show that UNR activates rather than represses elongation, at least of *VIM* and *RAC1* mRNAs. Stimulation of translational elongation of these transcripts by UNR contributes to the malignant properties of melanoma cells. The precise molecular mechanism by which UNR promotes elongation, and how UNR activity is regulated during melanoma development, are important questions for future research.

A network analysis was performed to reveal UNR-regulated targets directly involved in melanoma progression. The results uncovered 15 UNR targets that have previously been implicated in melanoma progression. Among these we find important downstream effectors of driver oncogenes that contribute to melanoma cell survival, invasion, and metastasis. For instance, the c-Jun proto-oncogene is a transcription factor hyperactivated in malignant melanoma (reviewed in Kappelmann et al., 2014). Two of the most relevant downstream effectors of c-Jun are the tumor suppressor PTEN and the inflammatory factor CCL2 (c-Jun downregulates *PTEN* and upregulates *CCL2* to promote cell survival and metastasis [Hettinger et al., 2007; Qian et al., 2011; Wolter et al., 2008]). UNR does not target c-Jun directly, but downregulates *PTEN* and upregulates *CCL2* mRNAs, providing a post-transcriptional mimic of the transcriptional c-Jun effect. These transcripts constitute an RNA regulon coordinated by UNR.

Another RNA regulon is composed of the transcripts encoding *SDC4*, *RAC1*, *TRIO*, *TNC*, *FN1*, *CTTN*, and *VIM*. SDC4 is a transmembrane receptor that connects the extracellular matrix with intracellular signaling pathways (Elfenbein and Simons, 2013). SDC4, as well as the guanine exchange factor TRIO, activate the small GTPase RAC1, which relays signals to the cytoskeleton to modulate adhesion and migration. Indeed, the activation of these factors has been linked to metastatic melanoma (Feng et al., 2014; Krauthammer et al., 2012; Ridgway et al., 2010). TNC and FN1 are proteins of the extracellular matrix that also interact with SDC4 to modulate cell adhesion. TNC overexpression has been related with melanoma invasion and metastasis, while FN1 upregulation suppresses motility of melanoma cell lines (Novak et al., 2015; Shao et al., 2015). CTTN binds actin and is required for the formation of invadopodia in invasive tumoral cells (Ayala et al., 2008) whereas, as mentioned above, VIM is a component of intermediate filaments that preserves the mechanical integrity of cells during invasion (Satelli and Li, 2011). All of these factors are coordinately regulated by UNR in a direction consistent with invasion and metastasis: UNR promotes the translation of *RAC1*, *TRIO*, and *VIM* mRNAs and upregulates *SDC4*, *TNC*, and *CTTN* transcript levels, while it represses the translation of the *FN1* message. These results reveal RNA regulons coordinated by UNR to modulate invasion and metastasis.

In addition to melanoma genes regulated by UNR, the network shows extensive connections of UNR targets with a large proportion of melanoma genes not directly regulated by UNR. Some of these targets are involved in progression of other tumor types while others have not been shown to contribute to cancer. For instance, ADAM12 is a metalloprotease involved in restructuring cell-cell and cell-matrix interactions that is upregulated by UNR, but whose function in melanoma has not been addressed. It will be interesting to test the contribution of ADAM12 to the acquisition of melanoma cancerous traits.

In summary, our data identify an oncogenic function for UNR, uncover UNR targets and mechanisms of regulation, and provide a resource of potential melanoma biomarkers and therapeutic targets.

EXPERIMENTAL PROCEDURES

Normal and malignant melanocytic cells, molecular and cell biology techniques, list of oligonucleotides, high-throughput methods, and detailed computational analysis are described in Supplemental Experimental Procedures. All sequencing was performed on Illumina HiSeq2000 (single read, 50 nt) at either the EMBL or the CRG Genomics Core facilities.

Ethics Approvals

All experimental animal procedures were approved by the Institutional Ethics Committees (CEEA) of the PRBB, the CNIO, and the Instituto de Salud Carlos III, and met the guidelines of Catalonian (Catalan law 5/1995 and Decrees 214/97, 32/2007) and European (EU directives 86/609 and 2001-486) regulations, as well as the Standards for Use of Laboratory Animals A5388-01 (NIH).

Human tumor biopsies were obtained from the i+12 Biobank (RD09/0076/00118) of the Hospital 12 de Octubre and the Spanish Hospital Biobank Network, under ethical protocols approved by their Clinical Investigation Ethical Committees. Procedures with human melanocytes were approved by the Ethical Committees of the CNIO and the Hospital 12 de Octubre. All human samples were obtained after informed consent from the patient.

RNA-Seq

Gene expression differences between shUNR and shControl cells were measured using poly(A)$^+$ RNA-seq, except for histones, for which we used ribozero-treated total RNA-seq. Libraries were sequenced, mapped to the hg19 human genome using TopHat2, and analyzed for differential gene expression using Cuffdiff2 (Trapnell et al., 2013). The p value threshold for differential gene expression calling was set to 0.005.

iCLIP-Seq

iCLIP was performed as described by Konig et al. (2011). Libraries were sequenced, mapped using Bowtie2 (Langmead and Salzberg, 2012), and corrected for amplification bias. Peaks were called using HOMER (http://homer.

salk.edu/homer/) and motif analysis was performed using DREME (Bailey et al., 2011).

Ribosome Profiling

RP was performed according to Ingolia et al. (2012). Details on ribosome profiling data analysis including pre-processing mapping and centering, differential crude RPF, translational efficiency, and ribosome distribution calculations can be found in Supplemental Experimental Procedures.

ACCESSION NUMBERS

The ArrayExpress accession numbers for the RNA-seq, iCLIP-seq, and RP experiments are E-MTAB-3805, E-MTAB-3818, and E-MTAB-3815, respectively.

SUPPLEMENTAL INFORMATION

Supplemental Information includes Supplemental Experimental Procedures, five figures, seven tables, and two movies and can be found with this article online at http://dx.doi.org/10.1016/j.ccell.2016.10.004.

AUTHOR CONTRIBUTIONS

F.G. conceived the project. Experimental data were contributed as follows: D.O., G.T.C., D.C.-W., J.M.-U., M.G.-F., Figures 1, 2H, and 2I; S.G., Figures 5G and 6A, and S1; N.B., Figures 2D–2F, S2D–S2H, and 6B. L.W. performed all other experimental work and P.P. provided bioinformatics analysis of all high-throughput data. S.H., M.S.S., and F.G. supervised the project. L.W., P.P., and F.G. wrote the manuscript. All other authors edited the manuscript.

ACKNOWLEDGMENTS

We thank Laura Battle and Olga Coll for technical assistance with xenograft experiments, José Luis Rodríguez-Peralto and Pablo Ortiz-Romero (Anatomical Pathology and Dermatology Services at the Hospital 12 de Octubre) for tissue procurement, and Corine Bertolotto for Mel-ST cells. We thank the CRG and EMBL Genomics Facilities for high-throughput sequencing, and the CRG Protein Service for recombinant UNR expression. We are grateful to Anne Willis for the human UNR cDNA, to Jernej Ule and Elías Bechara for advice on iCLIP, and to Nick Ingolia, Sebastian Leidel, and Danny Nedialkova for advice on ribosome profiling. We thank Juan Valcárcel, Johan Tisserand, and Jesús García-Foncillas for useful discussions and comments on the manuscript. L.W. was supported by the Fonds National de la Recherche, Luxembourg, and cofunded by the Marie Curie Actions of the European Commission (FP7-COFUND) (Project Code 1072489). M.G.-F. was supported by a Juan de la Cierva fellowship from the Spanish Ministry of Economy and Competitiveness (MINECO). This work was supported by MINECO and the European Regional Development Fund (ERDF) under grant BFU2012-37135 and BFU2015-68741 to F.G., and Consolider CSD2009-00080 and TV'13-20131430 (Marató de TV3) grants to F.G. and M.S.S. We acknowledge support of the Spanish Ministry of Economy and Competitiveness, Centro de Excelencia Severo Ochoa 2013–2017, SEV-2012-0208 (to CRG) and SEV-2011-0191 (to CNIO).

Received: September 7, 2015
Revised: June 13, 2016
Accepted: October 3, 2016
Published: October 27, 2016

REFERENCES

Abaza, I., Coll, O., Patalano, S., and Gebauer, F. (2006). Drosophila UNR is required for translational repression of male-specific lethal 2 mRNA during regulation of X-chromosome dosage compensation. Genes Dev. *20*, 380–389.

Athanasiadis, E.I., Antonopoulou, K., Chatzinasiou, F., Lill, C.M., Bourdakou, M.M., Sakellariou, A., Kypreou, K., Stefanaki, I., Evangelou, E., Ioannidis, J.P., et al. (2014). A Web-based database of genetic association studies in cutaneous melanoma enhanced with network-driven data exploration tools. Database (Oxford) *2014*, http://dx.doi.org/10.1093/database/bau101.

Ayala, I., Baldassarre, M., Giacchetti, G., Caldieri, G., Tete, S., Luini, A., and Buccione, R. (2008). Multiple regulatory inputs converge on cortactin to control invadopodia biogenesis and extracellular matrix degradation. J. Cell Sci. *121*, 369–378.

Bailey, T.L. (2011). DREME: motif discovery in transcription factor ChIP-seq data. Bioinformatics *27*, 1653–1659.

Bathia, S., and Thompson, J.A. (2016). PD-1 blockade in melanoma: a promising start, but a long way to go. JAMA *315*, 1573–1575.

Bid, H.K., Roberts, R.D., Manchanda, P.K., and Houghton, P.J. (2013). RAC1: an emerging therapeutic option for targeting cancer angiogenesis and metastasis. Mol. Cancer Ther. *12*, 1925–1934.

Castello, A., Fischer, B., Hentze, M.W., and Preiss, T. (2013). RNA-binding proteins in Mendelian disease. Trends Genet. *29*, 318–327.

Cerami, E.G., Gross, B.E., Demir, E., Rodchenkov, I., Babur, O., Anwar, N., Schultz, N., Bader, G.D., and Sander, C. (2011). Pathway Commons, a web resource for biological pathway data. Nucleic Acids Res. *39*, D685–D690.

Chang, T.C., Yamashita, A., Chen, C.Y., Yamashita, Y., Zhu, W., Durdan, S., Kahvejian, A., Sonenberg, N., and Shyu, A.B. (2004). UNR, a new partner of poly(A)-binding protein, plays a key role in translationally coupled mRNA turnover mediated by the c-fos major coding-region determinant. Genes Dev. *18*, 2010–2023.

Darnell, R.B. (2010). RNA regulation in neurologic disease and cancer. Cancer Res. Treat. *42*, 125–129.

Darnell, J.C., Van Driesche, S.J., Zhang, C., Hung, K.Y., Mele, A., Fraser, C.E., Stone, E.F., Chen, C., Fak, J.J., Chi, S.W., et al. (2011). FMRP stalls ribosomal translocation on mRNAs linked to synaptic function and autism. Cell *146*, 247–261.

Dormoy-Raclet, V., Markovits, J., Malato, Y., Huet, S., Lagarde, P., Montaudon, D., Jacquemin-Sablon, A., and Jacquemin-Sablon, H. (2007). Unr, a cytoplasmic RNA-binding protein with cold-shock domains, is involved in control of apoptosis in ES and HuH7 cells. Oncogene *26*, 2595–2605.

Duncan, K., Grskovic, M., Strein, C., Beckmann, K., Niggeweg, R., Abaza, I., Gebauer, F., Wilm, M., and Hentze, M.W. (2006). Sex-lethal imparts a sex-specific function to UNR by recruiting it to the msl-2 mRNA 3' UTR: translational repression for dosage compensation. Genes Dev. *20*, 368–379.

Dutton-Regester, K., and Hayward, N.K. (2012). Reviewing the somatic genetics of melanoma: from current to future analytical approaches. Pigment Cell Melanoma Res. *25*, 144–154.

Elatmani, H., Dormoy-Raclet, V., Dubus, P., Dautry, F., Chazaud, C., and Jacquemin-Sablon, H. (2011). The RNA-binding protein Unr prevents mouse embryonic stem cells differentiation toward the primitive endoderm lineage. Stem Cells *29*, 1504–1516.

Elfenbein, A., and Simons, M. (2013). Syndecan-4 signaling at a glance. J. Cell Sci. *126*, 3799–3804.

Evans, J.R., Mitchell, S.A., Spriggs, K.A., Ostrowski, J., Bomsztyk, K., Ostarek, D., and Willis, A.E. (2003). Members of the poly (rC) binding protein family stimulate the activity of the c-myc internal ribosome entry segment in vitro and in vivo. Oncogene *22*, 8012–8020.

Feng, X., Degese, M.S., Iglesias-Bartolome, R., Vaque, J.P., Molinolo, A.A., Rodrigues, M., Zaidi, M.R., Ksander, B.R., Merlino, G., Sodhi, A., et al. (2014). Hippo-independent activation of YAP by the GNAQ uveal melanoma oncogene through a trio-regulated rho GTPase signaling circuitry. Cancer Cell *25*, 831–845.

Flaherty, K.T., Hodi, F.S., and Fisher, D.E. (2012). From genes to drugs: targeted strategies for melanoma. Nat. Rev. Cancer *12*, 349–361.

Friend, K., Campbell, Z.T., Cooke, A., Kroll-Conner, P., Wickens, M.P., and Kimble, J. (2012). A conserved PUF-Ago-eEF1A complex attenuates translation elongation. Nat. Struct. Mol. Biol. *19*, 176–183.

Futreal, P.A., Coin, L., Marshall, M., Down, T., Hubbard, T., Wooster, R., Rahman, N., and Stratton, M.R. (2004). A census of human cancer genes. Nat. Rev. Cancer *4*, 177–183.

Goroncy, A.K., Koshiba, S., Tochio, N., Tomizawa, T., Inoue, M., Watanabe, S., Harada, T., Tanaka, A., Ohara, O., Kigawa, T., et al. (2010). The NMR solution structures of the five constituent cold-shock domains (CSD) of the human UNR (upstream of N-ras) protein. J. Struct. Funct. Genomics *11*, 181–188.

Hennig, J., Militti, C., Popowicz, G.M., Wang, I., Sonntag, M., Geerlof, A., Gabel, F., Gebauer, F., and Sattler, M. (2014). Structural basis for the assembly of the Sxl-Unr translation regulatory complex. Nature *515*, 287–290.

Hettinger, K., Vikhanskaya, F., Poh, M.K., Lee, M.K., de Belle, I., Zhang, J.T., Reddy, S.A., and Sabapathy, K. (2007). c-Jun promotes cellular survival by suppression of PTEN. Cell Death Differ *14*, 218–229.

Horos, R., Ijspeert, H., Pospisilova, D., Sendtner, R., Andrieu-Soler, C., Taskesen, E., Nieradka, A., Cmejla, R., Sendtner, M., Touw, I.P., et al. (2012). Ribosomal deficiencies in Diamond-Blackfan anemia impair translation of transcripts essential for differentiation of murine and human erythroblasts. Blood *119*, 262–272.

Hussey, G.S., Chaudhury, A., Dawson, A.E., Lindner, D.J., Knudsen, C.R., Wilce, M.C., Merrick, W.C., and Howe, P.H. (2011). Identification of an mRNP complex regulating tumorigenesis at the translational elongation step. Mol. Cell *41*, 419–431.

Ingolia, N.T., Ghaemmaghami, S., Newman, J.R., and Weissman, J.S. (2009). Genome-wide analysis in vivo of translation with nucleotide resolution using ribosome profiling. Science *324*, 218–223.

Ingolia, N.T., Brar, G.A., Rouskin, S., McGeachy, A.M., and Weissman, J.S. (2012). The ribosome profiling strategy for monitoring translation in vivo by deep sequencing of ribosome-protected mRNA fragments. Nature Protocols *7*, 1534–1550.

Kanehisa, M., and Goto, S. (2000). KEGG: Kyoto Encyclopedia of Genes and Genomes. Nucleic Acids Res. *28*, 27–30.

Kanehisa, M., Goto, S., Sato, Y., Kawashima, M., Furumichi, M., and Tanabe, M. (2014). Data, information, knowledge and principle: back to metabolism in KEGG. Nucleic Acids Res. *42*, D199–D205.

Kappelmann, M., Bosserhoff, A., and Kuphal, S. (2014). AP-1/c-Jun transcription factors: regulation and function in malignant melanoma. Eur. J. Cell Biol. *93*, 76–81.

Konig, J., Zarnack, K., Rot, G., Curk, T., Kayikci, M., Zupan, B., Turner, D.J., Luscombe, N.M., and Ule, J. (2011). iCLIP—transcriptome-wide mapping of protein-RNA interactions with individual nucleotide resolution. J. Vis. Exp. http://dx.doi.org/10.3791/2638.

Krauthammer, M., Kong, Y., Ha, B.H., Evans, P., Bacchiocchi, A., McCusker, J.P., Cheng, E., Davis, M.J., Goh, G., Choi, M., et al. (2012). Exome sequencing identifies recurrent somatic RAC1 mutations in melanoma. Nat. Genet. *44*, 1006–1014.

Langmead, B., and Salzberg, S.L. (2012). Fast gapped-read alignment with Bowtie 2. Nat. Methods *9*, 357–359.

Liu, B., Han, Y., and Qian, S.B. (2013). Cotranslational response to proteotoxic stress by elongation pausing of ribosomes. Mol. Cell *49*, 453–463.

Mihailovic, M., Wurth, L., Zambelli, F., Abaza, I., Militti, C., Mancuso, F.M., Roma, G., Pavesi, G., and Gebauer, F. (2012). Widespread generation of alternative UTRs contributes to sex-specific RNA binding by UNR. RNA *18*, 53–64.

Mihailovich, M., Militti, C., Gabaldon, T., and Gebauer, F. (2010). Eukaryotic cold shock domain proteins: highly versatile regulators of gene expression. Bioessays *32*, 109–118.

Militti, C., Maenner, S., Becker, P.B., and Gebauer, F. (2014). UNR facilitates the interaction of MLE with the lncRNA roX2 during *Drosophila* dosage compensation. Nat. Commun. *5*, 4762.

Mitchell, S.A., Spriggs, K.A., Coldwell, M.J., Jackson, R.J., and Willis, A.E. (2003). The Apaf-1 internal ribosome entry segment attains the correct structural conformation for function via interactions with PTB and unr. Mol. Cell *11*, 757–771.

Morris, A.R., Mukherjee, N., and Keene, J.D. (2010). Systematic analysis of posttranscriptional gene expression. Wiley Interdiscip. Rev. Syst. Biol. Med. *2*, 162–180.

Novak, M., Leonard, M.K., Yang, X.H., Kowluru, A., Belkin, A.M., and Kaetzel, D.M. (2015). Metastasis suppressor NME1 regulates melanoma cell morphology, self-adhesion and motility via induction of fibronectin expression. Exp. Dermatol. *24*, 455–461.

Patel, G.P., Ma, S., and Bag, J. (2005). The autoregulatory translational control element of poly(A)-binding protein mRNA forms a heteromeric ribonucleoprotein complex. Nucleic Acids Res. *33*, 7074–7089.

Qian, B.Z., Li, J., Zhang, H., Kitamura, T., Zhang, J., Campion, L.R., Kaiser, E.A., Snyder, L.A., and Pollard, J.W. (2011). CCL2 recruits inflammatory monocytes to facilitate breast-tumour metastasis. Nature *475*, 222–225.

Ridgway, L.D., Wetzel, M.D., and Marchetti, D. (2010). Modulation of GEF-H1 induced signaling by heparanase in brain metastatic melanoma cells. J. Cell Biochem. *111*, 1299–1309.

Satelli, A., and Li, S. (2011). Vimentin in cancer and its potential as a molecular target for cancer therapy. Cell Mol. Life Sci. *68*, 3033–3046.

Schadendorf, D., Fisher, D.E., Garbe, C., Gershenwald, J.E., Grob, J.J., Halpern, A., Herlyn, M., Marchetti, M.A., McArthur, G., Ribas, A., et al. (2015). Melanoma. Nat. Rev. Dis. Primers *1*, 15003.

Schepens, B., Tinton, S.A., Bruynooghe, Y., Parthoens, E., Haegman, M., Beyaert, R., and Cornelis, S. (2007). A role for hnRNP C1/C2 and Unr in internal initiation of translation during mitosis. EMBO J. *26*, 158–169.

Shalgi, R., Hurt, J.A., Krykbaeva, I., Taipale, M., Lindquist, S., and Burge, C.B. (2013). Widespread regulation of translation by elongation pausing in heat shock. Mol. Cell *49*, 439–452.

Shannon, P., Markiel, A., Ozier, O., Baliga, N.S., Wang, J.T., Ramage, D., Amin, N., Schwikowski, B., and Ideker, T. (2003). Cytoscape: a software environment for integrated models of biomolecular interaction networks. Genome Res. *13*, 2498–2504.

Shao, H., Kirkwood, J.M., and Wells, A. (2015). Tenascin-C signaling in melanoma. Cell Adh. Migr. *9*, 125–130.

Sonenberg, N., and Hinnebusch, A.G. (2009). Regulation of translation initiation in eukaryotes: mechanisms and biological targets. Cell *136*, 731–745.

Thompson, J.F., Shaw, H.M., Hersey, P., and Scolyer, R.A. (2004). The history and future of melanoma staging. J. Surg. Oncol. *86*, 224–235.

Tinton, S.A., Schepens, B., Bruynooghe, Y., Beyaert, R., and Cornelis, S. (2005). Regulation of the cell-cycle-dependent internal ribosome entry site of the PITSLRE protein kinase: roles of Unr (upstream of N-ras) protein and phosphorylated translation initiation factor eIF-2alpha. Biochem. J. *385*, 155–163.

Trapnell, C., Hendrickson, D.G., Sauvageau, M., Goff, L., Rinn, J.L., and Pachter, L. (2013). Differential analysis of gene regulation at transcript resolution with RNA-seq. Nat Biotechnol. *31*, 46–53.

Triqueneaux, G., Velten, M., Franzon, P., Dautry, F., and Jacquemin-Sablon, H. (1999). RNA binding specificity of Unr, a protein with five cold shock domains. Nucleic Acids Res. *27*, 1926–1934.

Vaqué, J.P., Dorsam, R.T., Feng, X., Iglesias-Bartolome, R., Forsthoefel, D.J., Chen, Q., Debant, A., Seeger, M.A., Ksander, B.R., Teramoto, H., et al. (2013). A genome-wide RNAi screen reveals a Trio-regulated Rho GTPase circuitry transducing mitogenic signals initiated by G protein-coupled receptors. Mol. Cell *49*, 94–108.

Wan, Y., Qu, K., Zhang, Q.C., Flynn, R.A., Manor, O., Ouyang, Z., Zhang, J., Spitale, R.C., Snyder, M.P., Segal, E., et al. (2014). Landscape and variation of RNA secondary structure across the human transcriptome. Nature *505*, 706–709.

Wolter, S., Doerrie, A., Weber, A., Schneider, H., Hoffmann, E., von der Ohe, J., Bakiri, L., Wagner, E.F., Resch, K., and Kracht, M. (2008). c-Jun controls histone modifications, NF-kappaB recruitment, and RNA polymerase II function to activate the ccl2 gene. Mol. Cell Biol. *28*, 4407–4423.

Wurth, L., and Gebauer, F. (2015). RNA-binding proteins, multifaceted translational regulators in cancer. Biochim. Biophys. Acta *1849*, 881–886.